Neuron
Perspective

Dynamically Primed Synaptic Vesicle States: Key to Understand Synaptic Short-Term Plasticity

Erwin Neher[1,*] and Nils Brose[2]
[1]Membrane Biophysics Emeritus Group, Max Planck Institute for Biophysical Chemistry, Am Fassberg 11, 37070 Göttingen, Germany
[2]Department of Molecular Neurobiology, Max Planck Institute for Experimental Medicine, Hermann-Rein-Straße 3, D-37075 Göttingen, Germany
*Correspondence: eneher@gwdg.de
https://doi.org/10.1016/j.neuron.2018.11.024

Based on evidence that the docked and primed synaptic vesicle state is very dynamic, we propose a three-step process for the buildup of the molecular machinery that mediates synaptic vesicle fusion: (1) loose tethering and docking of vesicles to release sites, forming the nucleus of SNARE-complex assembly, (2) tightening of the complex by association of additional proteins, and partial SNARE-complex zippering, and (3) Ca^{2+}-triggered fusion. We argue that the distinction between "phasic synapses" and "tonic synapses" reflects differences in resting occupancy and stability of the loosely and tightly docked states, and we assign corresponding timescales: with high-frequency synaptic activity and concomitantly increased Ca^{2+}-concentrations, step (1) can proceed within 10–50 ms, step (2) within 1–5 ms, and step (3) within 0.2–1 ms.

Synaptic signaling between nerve cells is initiated by the presynaptic release of neurotransmitters, which is mediated by the successive processes of synaptic vesicle (SV) tethering, SV priming and concomitant membrane attachment (docking) at the active zone (AZ), and Ca^{2+}-triggered SV fusion. Like most other cellular membrane fusion events, the SV fusion reaction itself is executed by soluble N-ethylmaleimide-factor attachment receptor (SNARE) complexes, which are formed by Synaptobrevin on SVs and Syntaxin and SNAP-25 at the AZ plasma membrane. Ca^{2+}-triggering at synapses, mediated by the Synaptotagmins (Südhof, 2013, 2014) can transiently increase the SV fusion rate by many orders of magnitude. The processes leading up to SV fusion are tightly controlled by multiple soluble and AZ proteins that regulate SV docking and priming (e.g., Munc13s and CAPSs) (Wojcik and Brose, 2007)

Traditionally, electrophysiological analyses of neurotransmitter release at synapses have been interpreted in terms of AZ release sites, at which SVs are docked and primed and then fuse with a certain probability upon arrival of an action potential (AP) due to the concomitant increase in the intracellular Ca^{2+} concentration $[Ca^{2+}]_i$. In this regard, the docked and primed SV state has mostly been assumed as static and irreversible, but recent discoveries have provided a new perspective with evidence that even at rest the docked and primed SV states may be labile and very dynamic. In particular, the new results indicate that docked SVs fluctuate between a loosely docked and primed state (LS), in which SNARE complexes are only partially zippered, and a tightly docked and primed one (TS), in which zippering has progressed much further (Figure 1).

Synaptotagmin-1 (Syt-1) is the Ca^{2+} sensor that triggers synchronous SV fusion in response to an AP. A recent study on the "synchronizing" action of Syt-1 in AP-induced SV fusion (Chang et al., 2018) showed that transmitter release in Syt-1-deficient synapses is desynchronized, a phenotype that can be partially rescued by Syt-1 mutants that lack the ability to bind to membranes and/or to the SNARE fusion complex. Unlike rescue with wild-type (WT) Syt-1, these mutant Syt-1 variants support synchronous SV fusion only for AP stimuli that are preceded by another AP within a 10–50 ms time window. A parallel analysis of the ultrastructural correlates of these functional characteristics of mutant-Syt-1-expressing synapses revealed that the number of SVs within ~5 nm distance from the plasma membrane is increased within 10 ms after a first AP, but rapidly drops back again. Thus, only within a time window of 10–50 ms does the spatial distribution of SVs resemble that of synapses expressing WT Syt-1. The study led to the conclusion that Syt-1 does not only act as the Ca^{2+} sensor of SV fusion but has a second role in supporting tight SV attachment to the plasma membrane and priming, confirming a previously demonstrated role of Syt-1 in docking (Wang et al., 2011). The data are explained by the assumption that this "sync-docking" of SVs by Syt-1 is a constitutive function of wild-type Syt1, but is only partial and Ca^{2+}-dependent with the Syt-1 mutants tested. Surprisingly, sync-docking is restricted to an extremely short time window in the mutant, which roughly agrees with that of paired-pulse facilitation. Its onset happens in less than 10 ms. These new findings add an important kinetic aspect to recent morphological data on the different tethering and docking/priming states of SVs and their molecular underpinnings (Imig et al., 2014) as they indicate that, at least under the circumstances tested, there is a dynamic Ca^{2+}-dependent interchange between two primed SV states—tightly and loosely docked to the AZ membrane. As discussed below, many other findings indicate that, even in WT synapses, the equilibrium between the LS and TS states is hardly ever shifted completely to TS. Thus, a transient stabilization of TS may also happen under normal physiological conditions.

A second recent study highlighting the dynamic nature of the primed SV state (He et al., 2017) demonstrated "de-priming", i.e., a progressive loss of the primed SV state in the absence of the SNARE-regulating proteins Munc13-1 and Munc18-1. At

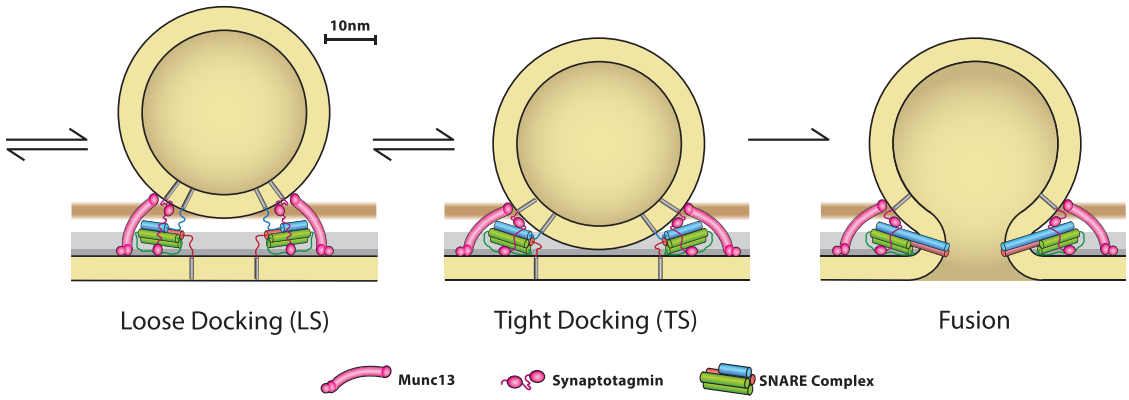

Figure 1. Graphic Representation of the Loosely and Tightly Docked/Primed SV States
SVs, membranes, and proteins are shown approximately at the same scale. The SV (45 nm in diameter) is placed at a membrane-to-membrane distance (8 nm) at which SNARES start to interact in a surface forces apparatus (Li et al., 2007) or form a loose complex in liposome studies (Yavuz et al., 2018).
Dark-gray shade: zone of tight docking/priming as defined by Imig et al. (2014).
Light-gray shade: zone of tight docking/priming as defined by Chang et al. (2018).
Brown shade: zone of increased SV density in docking/priming-defective mutants (Imig et al., 2014).
We do not claim correctness of the relative positions of proteins involved and would like to point out that only a subset of proteins present on SVs and at AZs is shown.

rest, only a very small primed SV pool can be generated when Munc13-1 is deleted so that only the low endogenous Munc13-2-levels are remaining, or else, when Munc18-1 is replaced by Munc18-2. In both cases, ongoing synaptic activity leads to a transient generation of a larger primed SV pool. A similar phenotype was seen previously upon the loss of CAPS-family SV primimg proteins (Jockusch et al., 2007). At rest, synaptic strength is very low in the corresponding mutants. Ongoing activity leads to strong facilitation due to an increasing releasable pool of SVs. This newly generated primed SV pool, however, is spontaneously deprimed within a time span of 10–50 s.

Together, these discoveries lead to the postulate that (1) the transmitter release machinery requires Munc13-1, Munc18-1, and SNAREs (and CAPSs; Jockusch et al., 2007; Imig et al., 2014), along with Syt-1, to tightly dock primed SVs to the AZ at the plasma membrane; that (2) in the absence of any of these proteins, SVs at rest relapse predominantly to a more spatially distant, loosely organized state with (partially) unzippered SNARE complexes; and that (3) this instability of the tightly docked and primed SV state can be compensated by increases in $[Ca^{2+}]_i$. Of note, though, the timescales of sync-docking and the spontaneous depriming of primed SVs are in the range of tens of ms in the former case and in the range of several seconds in the latter. Thus, a very steep Ca^{2+}-dependence of the underlying process must be postulated, or else it may be assumed that sync-docking senses microdomain $[Ca^{2+}]_i$, while the slow changes during and after repetitive activity reflect global $[Ca^{2+}]_i$.

Models of Vesicle Priming and Fusion

The aim of our perspective is to link these new findings to past literature on the mechanisms of SV priming and fusion, in particular with regard to electrophysiological studies on synaptic short-term plasticity (STP) and the possible molecular mechanisms involved. We point out accumulating electrophysiological evidence for extremely rapid reloading of primed SV pools during high-frequency synaptic activity and discuss how the molecular structures and rearrangements that take place during the buildup of the SV fusion machinery might support such rapid reloading processes. We posit that the speed of the reloading of the release-ready SV pool can be explained as the rapid transition between a loosely structured release machinery, the loosely docked state (LS), and a fully primed, tightly docked state (TS). We assign timescales to the various processes involved and argue that the labile nature of LS and TS, depending on the molecular composition, may be the feature that distinguishes so-called "phasic synapses" from "tonic synapses" (Atwood and Karunanithi, 2002).

In electrophysiological investigations, the concept of special SV release sites, the number of which is typically constant during the time span of experiments, has played a major role (Zucker, 1989). In the simplest possible reaction scheme, vesicles would dock to and be primed at such sites with a certain rate constant (which may be Ca^{2+} dependent) and then be released during APs or during experimentally induced increases in $[Ca^{2+}]_i$. Such increases in $[Ca^{2+}]_i$ can be accomplished to have a step-like time course (e.g., by step-like voltage-clamp depolarizations or by Ca^{2+} uncaging). For such stimuli and for such a minimum model it would be expected that a homogeneous population of vesicles would be released with an exponentially decaying time course. However, measured responses have almost invariably been shown not to decay with a single exponential. Rather, double-exponential or multi-exponential time courses were observed, indicating that the population of primed vesicles is heterogeneous, possibly with respect to the states they are in.

The adrenal chromaffin cell is arguably the secretory cell type on which these methods have been used most extensively (Pinheiro et al., 2016). In these cells, $[Ca^{2+}]_i$-jumps to 20–30 μM elicit an initial surge of fusion of chromaffin granules that decays with a time constant of 10-50 ms, followed by another ~10-fold slower fusion component (Rettig and Neher, 2002). The two components contribute about equally to total fusion and were initially interpreted to reflect two autonomously fusing granule

populations. However, subsequent studies (Voets et al., 1999) showed that when the rapidly fusing component is depleted after a strong stimulus, its recovery is accompanied by a transient decrease of the slowly fusing one. This indicates that the former recovers at the expense of the latter, or that vesicles transit from an upstream state to the releasable state. Later work (Walter et al., 2013) demonstrated that the data can be interpreted very well by assuming only one release-competent state of granules, which is depleted during the initial fusion surge and replenished from a feeding pool, which itself depletes on the hundreds-of-milliseconds timescale during prolonged stimulation. The two pools of granules may be seen as two states in analogy to the LS and TS states postulated above.

Numerous investigations of proteins and mechanisms involved in tethering, docking, and fusion of chromaffin granules have been conducted (Becherer and Rettig, 2006), but one finding seems to be particularly important for our discussion of functional aspects below: chromaffin cells do not display any signs of an upper bound to the number of release-ready granules—contrary to the evidence on synaptic vesicle fusion, which led to the postulate of a fixed number of SV fusion sites in synapses. Rather, what appears to be the releasable pool of chromaffin granules, such as the total number of granules that fuse upon a Ca^{2+}-uncaging flash (corresponding to the sum of LS and TS vesicles), depends in its size on the $[Ca^{2+}]_i$-level before the stimulus. This may be explained by a $[Ca^{2+}]_i$-dependent formation and decay of LS and TS. The lack of evidence for an upper bound to the sizes of LS and TS pools may indicate that typical AZ-like structures, which have not been documented for chromaffin cells, are not required for docking and priming of dense-core granules.

Compared to chromaffin cells, and in accord with the notion of a limited and constant number of SV fusion sites in synapses, the number of readily-releasable SVs in the Calyx of Held—the nerve terminal best-studied by voltage clamp depolarization and Ca^{2+} uncaging—is much less influenced by pre-stimulus $[Ca^{2+}]_i$. Yet, responses to voltage-clamp depolarization display multiple kinetic components: a component of rapidly fusing SVs, fusing within ~2–5 ms during stimulation with maximal Ca^{2+} current, and a slowly fusing SV pool, fusing in the tens-of-milliseconds range (Schneggenburger et al., 2002). After strong stimulation the rapidly fusing SV pool refills at the expense of the slowly fusing one (Lee et al., 2012), as had been shown for chromaffin cells. Importantly, the speed of transition between the two states is strongly reduced after preincubation with latrunculin, which depolymerizes actin networks (Lee et al., 2012; Miki et al., 2016). Studies on other giant nerve terminals, such as cerebellar mossy fibers (Hallermann et al., 2010; Ritzau-Jost et al., 2014), and on invertebrate neuromuscular junctions (Pan and Zucker, 2009) led to similar conclusions and were described by kinetic schemes that include two states of priming: a first, fast, initial priming step, generating SVs with low release probability, followed by a second, slow priming step that renders SVs more stimulus responsive and results in high-release probability. At least two, if not three (Taschenberger et al., 2016), SV states had to be postulated to explain corresponding data, except for one study on inhibitory synapses (Sakaba, 2008), where the data could be well described by assuming release from a single, homogeneous pool of SVs. In most cases, model calculations and fluctuation analyses (Hallermann et al., 2010; Hosoi et al., 2007; Miki et al., 2016; Pan and Zucker, 2009; Ritzau-Jost et al., 2014) were compatible with the assumption of a fixed number of SV fusion sites, to which release-ready SVs can bind in functionally heterogeneous states. Common to most of these studies is the assumption of a sequential arrangement of vesicle states. Most of them assigned release competence to at least two states with either $[Ca^{2+}]_i$-dependent or $[Ca^{2+}]_i$-independent transition rates between states.

Thus, there is substantial evidence in the electrophysiological literature that supports the postulate that SVs exist in two functional states and the notion of a sequential progression of SVs along a linear reaction coordinate. The novel aspect of the scheme proposed here is the emphasis on the postulate that the tightly docked SV state (TS) is only partially occupied at rest, that TS and LS states are mutually exclusive, and that release occurs mainly from TS. From a molecular point of view, the postulate that only vesicles in TS can fuse rapidly during an AP may seem reasonable. However, a recent report on a glutamatergic synapse in the cerebellum (Miki et al., 2018) indicated that, under certain circumstances, both SV priming (i.e., the LS→TS transition, as discussed here) and fusion may happen in short succession. It was found that release events are very well synchronized during a single AP. Yet, during high-frequency trains of stimulation, the latency distribution of release events during and after APs developed a second, slow component with a decay time constant of about 1.8 ms. Likewise, more than a doubling of the half-width of release transients during 100 Hz stimulus trains (from 0.42 to 0.99 ms) was reported in a study on the Calyx of Held (Scheuss et al., 2007). In an earlier study, a similar desynchronization of release was attributed to broadening of the microdomain $[Ca^{2+}]_i$ transient (Fedchyshyn and Wang, 2007). Thus, it seems that the LS→TS transition followed by SV fusion can occur in rapid succession, when $[Ca^{2+}]_i$ transients evoked by APs are lengthened.

The following discussion will assume a minimum-type reaction scheme, in which a given synapse has a fixed number of SV fusion sites, each of which can be empty or occupied by an SV in either the LS or the TS state, where only SVs in TS appear as "tightly docked" in electron microscopic images and SV fusion occurs predominantly from TS. Results will be discussed in terms of the quantities p_{TS} and p_{LS}, the probabilities that an SV at a fusion site is in the TS or LS, respectively. Regarding the use of the terms "docking" and "priming," we assume that these two processes have two aspects each, i.e., molecularly, the formation of loosely and tightly assembled SNARE-complexes, and morphologically, the absence or presence of SVs at distances < 5 nm from the AZ membrane. Future work will have to show whether and how the literature data quoted relate to the states of the minimum model, as suggested here.

Phasic and Tonic Synapses

The results summarized above reflect the situation at so-called "phasic synapses," synapses that either show "Short-Term Depression" (STD) during high-frequency trains of stimuli or a sequence of slight facilitation, followed by depression after 2–3 stimuli. An important mechanism of STD is the depletion of

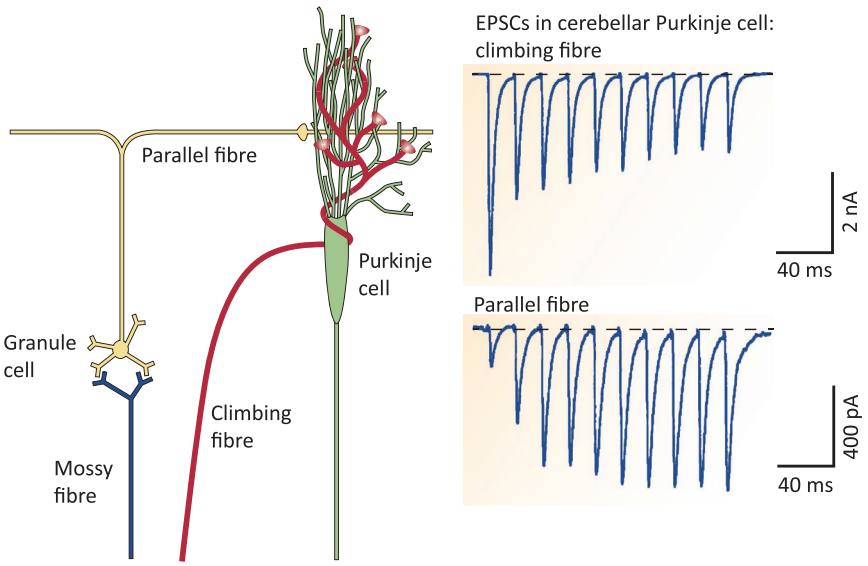

Figure 2. Two Representative Examples of Different Forms of Short-Term Synaptic Plasticity
Left: connectivity in the cerebellum.
Right, top: short-term depression at the cerebellar climbing fiber to Purkinje cell synapse—a typical "phasic" synapse.
Right, bottom: frequency facilitation at the parallel fiber to Purkinje cell synapse—a typical "tonic" synapse.
Adapted from Atwood and Karunanithi (2002) with permission.

a pool of rapidly fusing SVs during ongoing stimulation. In contrast, "tonic synapses" are initially weak after prolonged periods of rest, but their SV fusion capacity increases with each stimulus upon medium-frequency stimulation until postsynaptic responses reach about 10 times (in some cases 100 to 1,000 times) the size of the initial response (Figure 2). Striking examples of this synapse type are the tonic synapses of the crayfish neuromuscular junction (Atwood and Karunanithi, 2002; Pan and Zucker, 2009), hippocampal mossy fiber terminals (Hallermann et al., 2003; Salin et al., 1996; Vyleta and Jonas, 2014), and cerebellar granule cell to Purkinje cell synapses (Brachtendorf et al., 2015; Doussau et al., 2017).

We argue that a major contributor to the increase in synaptic strength of tonic synapses—beyond increases in release probability—is a rapid increase in occupancy of LS and TS, including a shift of SVs from LS to TS (i.e., into the tightly assembled state, see above), from which they fuse in response to an AP with high probability. Several findings support this hypothesis: (1) evidence that p_{TS} can be much smaller than 1 in certain synapses (see below); (2) evidence that molecular perturbations, such as certain Syt-1 mutations (Chang et al., 2018), or the lack of certain isoforms of synaptic proteins (He et al., 2017) lead to labile primed SV states, resulting in "tonic-like" STP; (3) evidence that the marked differences between phasic and tonic synapses at the crayfish neuromuscular junction can be modeled by postulating a labile pool of fusion-ready SVs (at rest) for tonic synapses and a more stable one for phasic ones (Pan and Zucker, 2009); and (4) evidence for a rapid transition between a "reluctantly releasable" and a "fully releasable" state of SVs (Lee et al., 2012; Miki et al., 2016; Ritzau-Jost et al., 2014; Saviane and Silver, 2006). An explanation of how differences in the stability of primed SV states, together with $[Ca^{2+}]_i$-dependent rate constants, translate into differences in p_{TS}, leading either to facilitation or depression, is presented in Figure 3. A recent study (Pulido and Marty, 2018) explores in detail how variations in rate constants lead to either facilitation or depression in simple and two-state SV docking site models.

Partial Occupancy of Release Sites

A p_{TS}<1 in resting synapses was found not only at typical tonic synapses but also at synapses that qualify as phasic. For instance, a detailed study of transmitter release-statistics at synapses between parallel fibers and molecular layer interneurons in the cerebellum, focusing on trains of high-frequency stimulation, could explain the observed time course of quanta released and its variance only when assuming a resting site occupancy of 0.45 for the release-ready SV state (Miki et al., 2016) (i.e., SVs in the TS according to our model). Likewise, a minimal stimulation study on GABAergic synapses (Pulido et al., 2015) resulted in the same low estimate for site occupancy. A synapse with p_{TS} = 0.45 may show either paired-pulse facilitation or paired-pulse depression, since the ratio of the first two response amplitudes in a stimulus train represents a balance of at least three processes: consumption of TS SVs during the first stimulus, reformation of TS SVs, and possibly an increase in release probability of TS SVs due to $[Ca^{2+}]_i$- buildup and/or Ca^{2+}-current facilitation (Borst and Sakmann, 1998; Neher, 2017). The smaller p_{TS} is at rest, the more likely TS SV reformation will dominate and lead to paired-pulse facilitation or a tonic character of release. Low p_{TS} also allows synapses to transiently overfill the TS pool relative to the resting state during periods of elevated $[Ca^{2+}]_i$, resulting in augmentation-like time courses of EPSCs after high-frequency stimulation.

In some tonic synapses, a 100- to 1,000-fold facilitation of transmitter release can be observed with repetitive stimulation (Millar et al., 2005). Based on our postulate that this facilitation reflects mainly changes in occupancy of the TS, a 100-fold facilitation implies that p_{TS} at rest cannot be larger than 0.01. For p_{TS} to increase during repetitive stimulation, the recruitment of SVs to the TS must be faster than SV loss due to exocytosis. Consequently, most studies on tonic synapses have postulated fast and strongly Ca^{2+}-dependent rates of SV priming into the releasable state (Brachtendorf et al., 2015; Doussau et al., 2017; Millar et al., 2005; Pan and Zucker, 2009). A detailed study on many aspects of STP in cerebellar granule cell to Purkinje cell synapses (Doussau et al., 2017) postulated that, at low-stimulation frequency, a single AP depletes the "fully releasable pool" of SVs by ~60%. Subsequently, a Ca^{2+}-activated surge of priming actually overfills this SV pool by up to ~180% (relative to the resting state) before the filling state drops back again with a

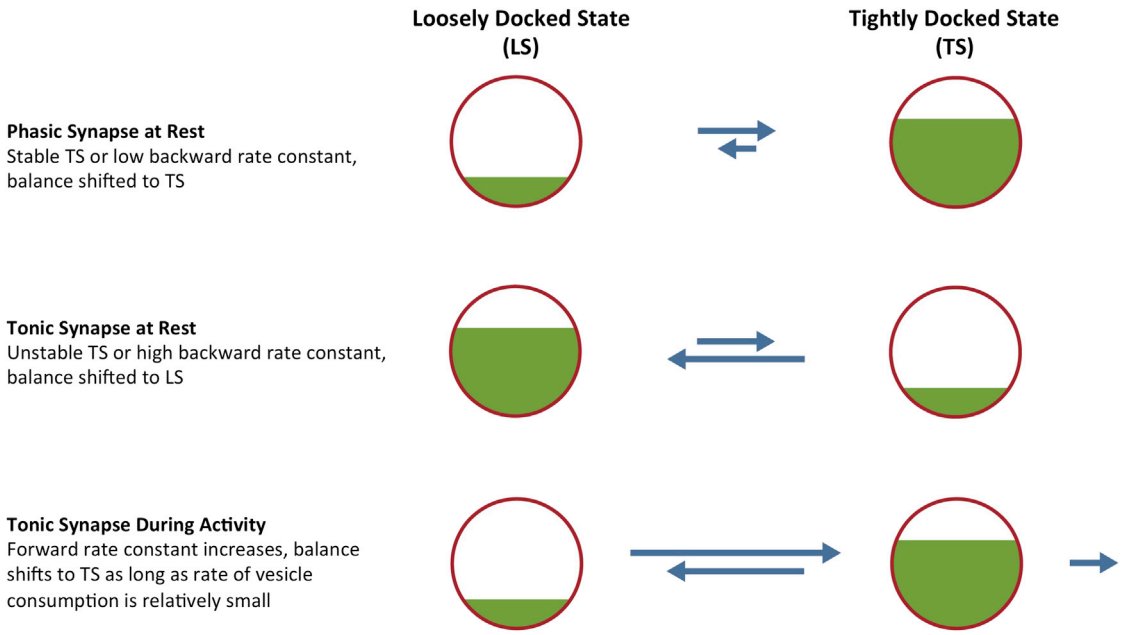

Figure 3. Stability of the Tightly Docked/Primed SV State and Frequency Facilitation
The circles represent SV pools, the colored portion indicating the degree of pool filling. Lengths of arrows indicate rate constants. In a phasic synapse, the rate constant for the LS→TS transition is larger than the reverse one. The tightly docked/primed pool fills up. In a tonic synapse this does not happen, because SVs de-prime due to a large de-priming rate – even if priming is as fast as in the former case. Frequency facilitation (filling-up of the TS) can happen if, upon activity, the LS→TS transition speeds up, as long as SV fusion (small arrow to the right) does not dominate the balance. During strong stimulation, TS SVs are consumed faster than they are supplied, resulting in depletion of the TS and LS and short-term depression.

time constant of about 75 ms (Doussau et al., 2017). This is two to three orders of magnitude faster than both the "de-priming" discussed above for hippocampal neurons expressing Munc13-2 and the decay of augmentation-like responses in phasic synapses to be discussed below. However, it is remarkably similar to the postulated time course of SV movement in Syt-1 mutant cells as assessed by electron microscopic analyses of synapses at different time intervals after AP stimulation (Chang et al., 2018). Similarly, experiments on a phasic synapse in the cerebellum (Miki et al., 2016) led to the related conclusion that paired-pulse facilitation at this synapse is largely due to transient overfilling of the releasable SV pool after a first action potential.

In summary, studies on both phasic and tonic synapses document a very dynamic fusion-competent SV pool – the TS in our terminology – and indicate that the main difference between phasic and tonic synapses is their p_{TS}, which is in the range of 0.4-0.7 for phasic synapses and $\leq$ 0.2 for tonic ones. Complementary studies on the molecular mechanisms that govern SV priming indicate that different stabilities of the TS due to variations in the de-priming rate may be major causes for this distinction. As shown (He et al., 2017) the lability of the fully primed TS state is determined by the molecular composition of the SV fusion apparatus, and we would argue that at rest p_{TS} is the higher, the more Munc13-1 is expressed in a given synapse, and the lower, the more Munc13-2 is present, at least in cultured hippocampal neurons, where the effects of Munc13s on STP seem to dominate. Adrenal chromaffin cells, which display very large increases in the exocytotic burst with increased pre-stimulus $[Ca^{2+}]_i$, fit very well into this scheme, since they express mainly Munc13-2 (Man et al., 2015). Likewise, the presence of CAPSs or different Munc18 paralogs may shift a given synapse along the tonic-phasic axis (Figure 4). However, the phasic/tonic character of synapses may also be influenced by other factors, since the loss of Munc13-2 in hippocampal mossy fiber terminals seems to enhance the tonic nature of these synapses (Breustedt et al., 2010).

Implications of Rapid Interconversion between Vesicle States

Common to all findings discussed above—or to our interpretation thereof—is the existence of at least two functional SV states, one of which fuses with high probability during an AP, and the other representing a precursor state that can be converted rapidly to the releasable state during synaptic activity and concomitant increases in $[Ca^{2+}]_i$. The existence of two (or more) functional SV states is not surprising from a molecular point of view, as the assembly of the SV fusion machinery is a complex process involving many components (Sørensen, 2009; Xu et al., 2017), and ultrastructural data document that distinct states of tethering and membrane attachment/docking of SVs are determined by SNARE proteins and a defined set of SNARE-regulating SV priming proteins (Imig et al., 2014).

The postulate that SNARE complexes may exist in a dynamic equilibrium between a loose and a tight state was put forward as early as 1999 (Xu et al., 1999) on the basis of the differential susceptibility of SNARE proteins to proteolysis by clostridial toxins. The surprising feature is that the conversion between the LS and

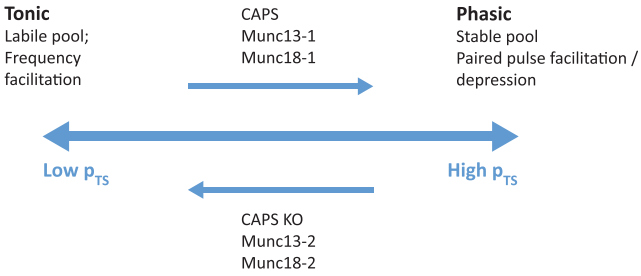

Figure 4. The Tonic/Phasic Axis

Synapse types can be arranged along an axis, representing the probability of docked/primed SVs adopting the tight state (p_{TS}). Tonic synapses are postulated to have low p_{TS}. Typical examples are tonic synapses of the crayfish neuromuscular junction, hippocampal mossy fiber terminals, and cerebellar granule cell to Purkinje cell synapses. Phasic ones are postulated to have high p_{TS}, such as phasic synapses of the crayfish neuromuscular junction, cerebellar mossy fiber terminals, and the Calyx of Held synapse.

TS states of SVs appears to be extremely fast during sustained high-frequency synaptic activity and concomitant increases in $[Ca^{2+}]_i$ (Lee et al., 2012; Miki et al., 2016; Ritzau-Jost et al., 2014; Saviane and Silver, 2006). Reinterpreting such data in terms of the minimum model proposed here indicates that the conversion in some cases can happen within 1 to only a few ms. This has important consequences for the molecular interpretation of electrophysiological data, since current methods of measuring the size of readily-releasable SV pools (Neher, 2015) do not allow a discrimination between TS and LS SVs if their interconversion occurs at the ms timescale. Rather, pool estimates will report the sum of the two so that the release probabilities, calculated as the ratio of EPSC amplitude versus pool size, will be the product $p_A \times p_{TS}/(p_{TS} + p_{LS})$, where p_A is the probability of an SV in TS to fuse during an AP. Thus, the estimate for release probability, which is generally regarded to represent the $[Ca^{2+}]_i$-dependent triggering of SV fusion, includes the LS-TS equilibrium, i.e., an SV priming step that is also regulated by $[Ca^{2+}]_i$. Accordingly, studies on Ca^{2+}-channel-SV coupling based on the action of Ca^{2+}-buffers need to be interpreted with caution. They usually assume that changes in "release probability," which are observed after addition of buffers, are only influenced by changes in AP-induced microdomains of elevated $[Ca^{2+}]_i$ near voltage-gated Ca^{2+} channels. However, they may also be influenced by changes in resting $[Ca^{2+}]_i$, modulating p_{TS}, unless care is taken that addition of buffers does not change resting $[Ca^{2+}]_i$. In essence, more refined stimulation protocols will be required to tease apart changes in p_{TS} and p_A and to obtain insight into the mechanisms that control them. Such studies will have to take into account the well-known, strong influence of Ca^{2+}-current magnitude and duration as well as of the spatial coupling between channels and release sites on p_A (Nakamura et al., 2015).

Ultrastructural and Molecular Manifestations of Different SV Priming States

Recent electron microscopic data (Imig et al., 2014) showed that a total blockade of SV priming upon deletion of Munc13-family SV priming proteins—causing a complete loss of all primed SVs—leads to a loss of membrane attached SVs (≤1.6 nm distance from the AZ membrane), a strong reduction in the number of SVs at ~2–4 nm distance from the AZ membrane, and an accumulation of SVs at ~8–10 nm distance from the AZ. Similar observations were made in the absence of synaptic SNARE proteins. These data indicate that Munc13-family proteins and SNARE proteins are necessary for the formation of the TS. They imply in the framework of the considerations outlined above that primed LS and TS SVs have at least partially engaged trans-SNARE complexes and are linked to the AZ membrane at a distance of at most 8 nm (see Figure 1 for a graphical representation of LS and TS). This interpretation is in accord with findings indicating that trans-SNARE complex engagement requires an inter-membrane distance of at most 8 nm (Li et al., 2007; van den Bogaart et al., 2011; Yavuz et al., 2018). Furthermore, the recent ultrastructural study of Syt-1-deficient synapses before and after stimulation discussed above (Chang et al., 2018) correlated the absence and $[Ca^{2+}]_i$/Syt-1-dependent rescue of a synchronously fusing, primed SV pool with a partial loss and $[Ca^{2+}]_i$/Syt-1-dependent recovery of SVs at ~0–5 nm distance from the AZ plasma membrane. $[Ca^{2+}]_i$-dependence, rather than any other effect of stimulation, was implicated by the finding that intact $[Ca^{2+}]_i$-binding sites of Syt-1 are required for the described effects. We postulate that these rapidly recovering SVs are bound to release sites at rest in the LS-configuration. This allows them to reside more than 5 nm away from the AZ. Upon an increase in $[Ca^{2+}]_i$ they transit to the TS within a few ms, implying a move of about 5 nm. This fast LS→TS transition would be possible if LS SVs had already partially engaged SNARE complexes so that the most time consuming steps in exocytosis (i.e., bringing t-SNARE and v-SNARE motifs into register at their N-terminal ends (Sitarska et al., 2017) and establishing the correct sub-configurations; Lai et al., 2017) have already taken place during the formation of the LS. What may be the timescale of *de-novo* LS formation? Presumably it is determined by the rate-limiting steps observed in electrophysiological experiments employing high-frequency train stimulation at steady-state. Replacement SVs (Miki et al., 2016) or SVs with low fusion probability (Miki et al., 2016; Ritzau-Jost et al., 2014) are resupplied under such conditions within 20–50 ms (i.e., at a ~10-fold slower rate than the rate of the LS→TS transition).

Molecular Mechanisms Involved in the LS→TS Transition

A discussion of presynaptic proteins involved in the LS→TS transition must currently remain speculative. This is due in large part to the fact that the majority of genetic perturbations of presynaptic proteins assessed to date cause changes in release probability and STP, indicating that these parameters are subject to a plethora of direct and indirect influences by numerous proteins. However, in view of the recent studies that motivated our perspective (He et al., 2017; Chang et al., 2018) and because electrophysiological experiments show that the LS→TS transition is dramatically accelerated by synaptic activity—and consequent changes in $[Ca^{2+}]_i$—Synaptotagmins and Munc13s are particularly interesting candidates as both are regulated by $[Ca^{2+}]_i$-dependent processes and play a role in SV priming. Indeed, Munc13s are particularly well suited to control the

LS→TS transition because they are dedicated and absolutely essential SV priming proteins and because their activity is regulated in a very complex manner by multiple $[Ca^{2+}]_i$-dependent processes, suggesting that neurons in fact "use" Munc13s purposively to regulate the LS→TS transition.

The combined ultrastructural and functional changes observed in Syt-1-deficient synapses and the structural Syt-1 features that are required to revert these changes in rescue experiments (Chang et al., 2018) indicate that Syt-1 itself may affect the LS→TS equilibrium of SVs by stabilizing the TS via interactions of its C2B domain with membrane lipids (Bai et al., 2004; Brewer et al., 2015; Honigmann et al., 2013; van den Bogaart et al., 2011; Xue et al., 2008). Syt-1 mediates $[Ca^{2+}]_I$ dependence of the sync-docking effect via its $[Ca^{2+}]_i$-sensing loops (Chang et al., 2018), which are known to sense the high and short-lived $[Ca^{2+}]_I$ microdomain signals generated by APs. Together with the low Ca^{2+} affinity of these sites (implying short Ca^{2+} occupancy), such properties may explain the very short duration of sync-docking after APs. A similar mechanism may boost the LS→TS transition during and after phases of ongoing synaptic activity and concomitant moderate increases in $[Ca^{2+}]_i$, but this would require Ca^{2+}-binding sites with higher affinity (see below).

Syt-7 has been postulated to be the Ca^{2+}-sensor for facilitation, based on studies on several types of synapses, at which facilitation is reduced upon Syt-7 knock-out (Jackman et al., 2016). The findings were interpreted in terms of a block of an increase in release probability during repetitive stimulation (Jackman and Regehr, 2017). However, given the ideas propagated here, the changes in "apparent" release probability may also be due to an influence on the LS→TS transition, i.e., a change in SV priming, which would be more in line with an earlier study on the role of Syt-7 in STP and priming (Liu et al., 2014).

Beyond Synaptotagmin-related processes, Ca^{2+} binding to SV priming proteins of the Munc13 family may contribute to the LS→TS transition. As mentioned above, Munc13s are absolutely essential for SV priming, so that their genetic deletion leads to a total loss of all primed (i.e., LS and TS) SVs and a total shut-down of SV fusion (Sigler et al., 2017; Varoqueaux et al., 2002). Probably most importantly in the present context, Munc13 function is controlled by two fast-acting, Ca^{2+}-dependent regulatory processes involving Ca^{2+}/Calmodulin (Junge et al., 2004; Lipstein et al., 2013) and Ca^{2+}/PIP_2 (Shin et al., 2010), which operate at low and high $[Ca^{2+}]_i$, respectively. Multiple genetic perturbation studies showed that Munc13s exert dynamic changes in SV fusion characteristics over a wide timescale, including strong effects on release probability and STP during high-frequency stimulation trains. In cultured hippocampal neurons, for instance, the inactivation of Ca^{2+}/Calmodulin binding to Munc13s or of Ca^{2+}/PIP_2 binding to the C2B domain has profound effects on STP, which shifts toward a more "phasic" character (Junge et al., 2004; Shin et al., 2010). Furthermore, Munc13 function is regulated by diacylglycerol-binding to a C1 domain that directly flanks the central C2B domain, and phorbol esters acting upon the C1 domain, mimicking diacylglycerol, enhance SV fusion and lead to increased synaptic depression (Rhee et al., 2002). A gain of function mutation in the Munc13-1 C1 domain causes a massive shift toward phasic STP characteristics, which becomes manifest as an increased release probability, a reduced paired-pulse ratio, and a strongly increased synaptic depression during 10 Hz stimulation (Basu et al., 2007; Rhee et al., 2002). Accordingly, a study on the Munc13-1 ortholog in *C. elegans* (Michelassi et al., 2017) demonstrated an autoinhibitory action of C1 and C2 domains upon Unc-13 activity and SV priming, which is relieved by genetic elimination of the respective domains, or by DAG/phorbol ester binding and Ca^{2+}/PIP_2 binding to the C1 and C2B domain, respectively. In terms of the two-step SV priming scheme proposed here, the intact regulatory "apo-domains" of Munc13s would partially impede the formation of TS, while ligand binding to the C1 and C2B domains would allow for a shift of the LS-TS equilibrium toward TS. The enhanced depression during stimulation would then reflect the rapid depletion of TS SVs.

Overall, the available data on Munc13s indicate that these key SV-priming proteins do not only control basic SV priming into the LS state but may also be used by neurons in a purposive manner to control activity-dependent LS→TS transitions, where Ca^{2+}/Calmodulin-, Ca^{2+}/PIP_2-, and diaycylglycerol-signaling may lead to conformational changes in the structure of Munc13s bound to SNARE-complexes that promote progression to the TS state. Allosteric interactions within the whole SV-fusion apparatus may combine regulatory effects of Munc13s with those of Synaptotagmins to generate activity-dependent STP over a wide timescale and a broad $[Ca^{2+}]_i$ range.

Conclusion

We propose that SV fusion and the release of neurotransmitters should be considered a three-step process: (1) initial loose docking and priming of SVs at AZ release sites and the buildup of a loosely organized fusion machinery (LS), which occurs on the timescale of ~20–50 ms upon high-frequency synaptic activity and the concomitantly increased $[Ca^{2+}]_I$; (2) a reversible transition to the tightly docked state (TS), which is slow at rest, but can happen within ~1–5 ms at high $[Ca^{2+}]_I$; and (3) Ca^{2+}-triggered SV fusion with sub-millisecond kinetics.

In this scenario, synapses may be categorized along an axis that defines their probability of TS occupancy (p_{TS}) at rest (Figure 4). At the low-p_{TS} end of this axis are synapses that have traditionally been designated as tonic, while the other end of the axis represents phasic synapses, such as the classical CA3-CA1 synapses of the hippocampus or those of the vertebrate neuromuscular junction. It should be noted that p_{TS} in this context is the probability of finding an SV in state TS, not that of occupancy of a given release site. The very low EPSCs of some tonic synapses, however, may indicate that it is not only a shift from TS to LS that limits SV fusion after periods of rest, but also a near-complete loss of SVs from release sites altogether. We would like to emphasize that the scheme we propose here should be considered tentative and as a minimum-type model. Quantitative kinetic analysis of electrophysiological data will be required in order to determine to what extent they are compatible with our interpretation and/or how the minimum model needs to be extended in order to explain short-term plasticity in a given type of synapse.

ACKNOWLEDGMENT

We acknowledge support by the European Commission, (ERC Advanced Grant SYNPRIME - REP-670283-2; N.B.). We are grateful to Alain Marty, Stefan Hallermann, Tomoyuki Takahashi, Christian Rosenmund, and Reinhard Jahn for numerous helpful comments on the manuscript.

REFERENCES

Atwood, H.L., and Karunanithi, S. (2002). Diversification of synaptic strength: presynaptic elements. Nat. Rev. Neurosci. *3*, 497–516.

Bai, J., Tucker, W.C., and Chapman, E.R. (2004). PIP2 increases the speed of response of synaptotagmin and steers its membrane-penetration activity toward the plasma membrane. Nat. Struct. Mol. Biol. *11*, 36–44.

Basu, J., Betz, A., Brose, N., and Rosenmund, C. (2007). Munc13-1 C1 domain activation lowers the energy barrier for synaptic vesicle fusion. J. Neurosci. *27*, 1200–1210.

Becherer, U., and Rettig, J. (2006). Vesicle pools, docking, priming, and release. Cell Tissue Res. *326*, 393–407.

Borst, J.G.G., and Sakmann, B. (1998). Facilitation of presynaptic calcium currents in the rat brainstem. J. Physiol. *513*, 149–155.

Brachtendorf, S., Eilers, J., and Schmidt, H. (2015). A use-dependent increase in release sites drives facilitation at calretinin-deficient cerebellar parallel-fiber synapses. Front. Cell. Neurosci. *9*, 27.

Breustedt, J., Gundlfinger, A., Varoqueaux, F., Reim, K., Brose, N., and Schmitz, D. (2010). Munc13-2 differentially affects hippocampal synaptic transmission and plasticity. Cereb. Cortex *20*, 1109–1120.

Brewer, K.D., Bacaj, T., Cavalli, A., Camilloni, C., Swarbrick, J.D., Liu, J., Zhou, A., Zhou, P., Barlow, N., Xu, J., et al. (2015). Dynamic binding mode of a Synaptotagmin-1-SNARE complex in solution. Nat. Struct. Mol. Biol. *22*, 555–564.

Chang, S., Trimbuch, T., and Rosenmund, C. (2018). Synaptotagmin-1 drives synchronous Ca^{2+}-triggered fusion by C_2B-domain-mediated synaptic-vesicle-membrane attachment. Nat. Neurosci. *21*, 33–40.

Doussau, F., Schmidt, H., Dorgans, K., Valera, A.M., Poulain, B., and Isope, P. (2017). Frequency-dependent mobilization of heterogeneous pools of synaptic vesicles shapes presynaptic plasticity. eLife *6*, e28935.

Fedchyshyn, M.J., and Wang, L.Y. (2007). Activity-dependent changes in temporal components of neurotransmission at the juvenile mouse calyx of Held synapse. J. Physiol. *581*, 581–602.

Hallermann, S., Pawlu, C., Jonas, P., and Heckmann, M. (2003). A large pool of releasable vesicles in a cortical glutamatergic synapse. Proc. Natl. Acad. Sci. USA *100*, 8975–8980.

Hallermann, S., Fejtova, A., Schmidt, H., Weyhersmüller, A., Silver, R.A., Gundelfinger, E.D., and Eilers, J. (2010). Bassoon speeds vesicle reloading at a central excitatory synapse. Neuron *68*, 710–723.

He, E., Wierda, K., van Westen, R., Broeke, J.H., Toonen, R.F., Cornelisse, L.N., and Verhage, M. (2017). Munc13-1 and Munc18-1 together prevent NSF-dependent de-priming of synaptic vesicles. Nat. Commun. *8*, 15915.

Honigmann, A., van den Bogaart, G., Iraheta, E., Risselada, H.J., Milovanovic, D., Mueller, V., Müllar, S., Diederichsen, U., Fasshauer, D., Grubmüller, H., et al. (2013). Phosphatidylinositol 4,5-bisphosphate clusters act as molecular beacons for vesicle recruitment. Nat. Struct. Mol. Biol. *20*, 679–686.

Hosoi, N., Sakaba, T., and Neher, E. (2007). Quantitative analysis of calcium-dependent vesicle recruitment and its functional role at the calyx of Held synapse. J. Neurosci. *27*, 14286–14298.

Imig, C., Min, S.W., Krinner, S., Arancillo, M., Rosenmund, C., Südhof, T.C., Rhee, J., Brose, N., and Cooper, B.H. (2014). The morphological and molecular nature of synaptic vesicle priming at presynaptic active zones. Neuron *84*, 416–431.

Jackman, S.L., and Regehr, W.G. (2017). The mechanisms and functions of synaptic facilitation. Neuron *94*, 447–464.

Jackman, S.L., Turecek, J., Belinsky, J.E., and Regehr, W.G. (2016). The calcium sensor synaptotagmin 7 is required for synaptic facilitation. Nature *529*, 88–91.

Jockusch, W.J., Speidel, D., Sigler, A., Sørensen, J.B., Varoqueaux, F., Rhee, J.S., and Brose, N. (2007). CAPS-1 and CAPS-2 are essential synaptic vesicle priming proteins. Cell *131*, 796–808.

Junge, H.J., Rhee, J.S., Jahn, O., Varoqueaux, F., Spiess, J., Waxham, M.N., Rosenmund, C., and Brose, N. (2004). Calmodulin and Munc13 form a Ca2+ sensor/effector complex that controls short-term synaptic plasticity. Cell *118*, 389–401.

Lai, Y., Choi, U.B., Leitz, J., Rhee, H.J., Lee, C., Altas, B., Zhao, M., Pfuetzner, R.A., Wang, A.L., Brose, N., et al. (2017). Molecular mechanisms of synaptic vesicle priming by Munc13 and Munc18. Neuron *95*, 591–607.e10.

Lee, J.S., Ho, W.K., and Lee, S.H. (2012). Actin-dependent rapid recruitment of reluctant synaptic vesicles into a fast-releasing vesicle pool. Proc. Natl. Acad. Sci. USA *109*, E765–E774.

Li, F., Pincet, F., Perez, E., Eng, W.S., Melia, T.J., Rothman, J.E., and Tareste, D. (2007). Energetics and dynamics of SNAREpin folding across lipid bilayers. Nat. Struct. Mol. Biol. *14*, 890–896.

Lipstein, N., Sakaba, T., Cooper, B.H., Lin, K.H., Strenzke, N., Ashery, U., Rhee, J.S., Taschenberger, H., Neher, E., and Brose, N. (2013). Dynamic control of synaptic vesicle replenishment and short-term plasticity by Ca(2+)-calmodulin-Munc13-1 signaling. Neuron *79*, 82–96.

Liu, H., Bai, H., Hui, E., Yang, L., Evans, C.S., Wang, Z., Kwon, S.E., and Chapman, E.R. (2014). Synaptotagmin 7 functions as a Ca2+-sensor for synaptic vesicle replenishment. eLife *3*, e01524.

Man, K.N.M., Imig, C., Walter, A.M., Pinheiro, P.S., Stevens, D.R., Rettig, J., Sørensen, J.B., Cooper, B.H., Brose, N., and Wojcik, S.M. (2015). Identification of a Munc13-sensitive step in chromaffin cell large dense-core vesicle exocytosis. eLife *4*, e10635.

Michelassi, F., Liu, H., Hu, Z., and Dittman, J.S. (2017). A C1-C2 module in Munc13 inhibits calcium-dependent neurotransmitter release. Neuron *95*, 577–590.e5.

Miki, T., Malagon, G., Pulido, C., Llano, I., Neher, E., and Marty, A. (2016). Actin- and Myosin-dependent vesicle loading of presynaptic docking sites prior to exocytosis. Neuron *91*, 808–823.

Miki, T., Nakamura, Y., Malagon, G., Neher, E., and Marty, A. (2018). Two-component latency distributions indicate two-step vesicular release at simple glutamatergic synapses. Nat. Commun. *9*, 3943.

Millar, A.G., Zucker, R.S., Ellis-Davies, G.C., Charlton, M.P., and Atwood, H.L. (2005). Calcium sensitivity of neurotransmitter release differs at phasic and tonic synapses. J. Neurosci. *25*, 3113–3125.

Nakamura, Y., Harada, H., Kamasawa, N., Matsui, K., Rothman, J.S., Shigemoto, R., Silver, R.A., DiGregorio, D.A., and Takahashi, T. (2015). Nanoscale distribution of presynaptic Ca(2+) channels and its impact on vesicular release during development. Neuron *85*, 145–158.

Neher, E. (2015). Merits and limitations of vesicle pool models in view of heterogeneous populations of synaptic vesicles. Neuron *87*, 1131–1142.

Neher, E. (2017). Some subtle lessons from the calyx of held synapse. Biophys. J. *112*, 215–223.

Pan, B., and Zucker, R.S. (2009). A general model of synaptic transmission and short-term plasticity. Neuron *62*, 539–554.

Pinheiro, P.S., Houy, S., and Sørensen, J.B. (2016). C2-domain containing calcium sensors in neuroendocrine secretion. J. Neurochem. *139*, 943–958.

Pulido, C., and Marty, A. (2018). A two-step docking site model predicting different short-term synaptic plasticity patterns. J. Gen. Physiol. *150*, 1107–1124.

Pulido, C., Trigo, F.F., Llano, I., and Marty, A. (2015). Vesicular release statistics and unitary postsynaptic current at single GABAergic synapses. Neuron *85*, 159–172.

Rettig, J., and Neher, E. (2002). Emerging roles of presynaptic proteins in Ca++-triggered exocytosis. Science *298*, 781–785.

Rhee, J.S., Betz, A., Pyott, S., Reim, K., Varoqueaux, F., Augustin, I., Hesse, D., Südhof, T.C., Takahashi, M., Rosenmund, C., and Brose, N. (2002). Beta phorbol ester- and diacylglycerol-induced augmentation of transmitter release is mediated by Munc13s and not by PKCs. Cell *108*, 121–133.

Ritzau-Jost, A., Delvendahl, I., Rings, A., Byczkowicz, N., Harada, H., Shigemoto, R., Hirrlinger, J., Eilers, J., and Hallermann, S. (2014). Ultrafast action potentials mediate kilohertz signaling at a central synapse. Neuron *84*, 152–163.

Sakaba, T. (2008). Two Ca(2+)-dependent steps controlling synaptic vesicle fusion and replenishment at the cerebellar basket cell terminal. Neuron *57*, 406–419.

Salin, P.A., Scanziani, M., Malenka, R.C., and Nicoll, R.A. (1996). Distinct short-term plasticity at two excitatory synapses in the hippocampus. Proc. Natl. Acad. Sci. USA *93*, 13304–13309.

Saviane, C., and Silver, R.A. (2006). Fast vesicle reloading and a large pool sustain high bandwidth transmission at a central synapse. Nature *439*, 983–987.

Scheuss, V., Taschenberger, H., and Neher, E. (2007). Kinetics of both synchronous and asynchronous quantal release during trains of action potential-evoked EPSCs at the rat calyx of Held. J. Physiol. *585*, 361–381.

Schneggenburger, R., Sakaba, T., and Neher, E. (2002). Vesicle pools and short-term synaptic depression: lessons from a large synapse. Trends Neurosci. *25*, 206–212.

Shin, O.H., Lu, J., Rhee, J.S., Tomchick, D.R., Pang, Z.P.P., Wojcik, S.M., Camacho-Perez, M., Brose, N., Machius, M., Rizo, J., et al. (2010). Munc13 C2B domain is an activity-dependent Ca2+ regulator of synaptic exocytosis. Nat. Struct. Mol. Biol. *17*, 280–288.

Sigler, A., Oh, W.C., Imig, C., Altas, B., Kawabe, H., Cooper, B.H., Kwon, H.B., Rhee, J.S., and Brose, N. (2017). Formation and maintenance of functional spines in the absence of presynaptic glutamate release. Neuron *94*, 304–311.e4.

Sitarska, E., Xu, J., Park, S., Liu, X., Quade, B., Stepien, K., Sugita, K., Brautigam, C.A., Sugita, S., and Rizo, J. (2017). Autoinhibition of Munc18-1 modulates synaptobrevin binding and helps to enable Munc13-dependent regulation of membrane fusion. eLife *6*, e24278.

Sørensen, J.B. (2009). Conflicting views on the membrane fusion machinery and the fusion pore. Annu. Rev. Cell Dev. Biol. *25*, 513–537.

Südhof, T.C. (2013). Neurotransmitter release: the last millisecond in the life of a synaptic vesicle. Neuron *80*, 675–690.

Südhof, T.C. (2014). The molecular machinery of neurotransmitter release (Nobel lecture). Angew. Chem. Int. Ed. Engl. *53*, 12696–12717.

Taschenberger, H., Woehler, A., and Neher, E. (2016). Superpriming of synaptic vesicles as a common basis for intersynapse variability and modulation of synaptic strength. Proc. Natl. Acad. Sci. USA *113*, E4548–E4557.

van den Bogaart, G., Thutupalli, S., Risselada, J.H., Meyenberg, K., Holt, M., Riedel, D., Diederichsen, U., Herminghaus, S., Grubmüller, H., and Jahn, R. (2011). Synaptotagmin-1 may be a distance regulator acting upstream of SNARE nucleation. Nat. Struct. Mol. Biol. *18*, 805–812.

Varoqueaux, F., Sigler, A., Rhee, J.S., Brose, N., Enk, C., Reim, K., and Rosenmund, C. (2002). Total arrest of spontaneous and evoked synaptic transmission but normal synaptogenesis in the absence of Munc13-mediated vesicle priming. Proc. Natl. Acad. Sci. USA *99*, 9037–9042.

Voets, T., Neher, E., and Moser, T. (1999). Mechanisms underlying phasic and sustained secretion in chromaffin cells from mouse adrenal slices. Neuron *23*, 607–615.

Vyleta, N.P., and Jonas, P. (2014). Loose coupling between Ca2+ channels and release sensors at a plastic hippocampal synapse. Science *343*, 665–670.

Walter, A.M., Pinheiro, P.S., Verhage, M., and Sørensen, J.B. (2013). A sequential vesicle pool model with a single release sensor and a Ca(2+)-dependent priming catalyst effectively explains Ca(2+)-dependent properties of neurosecretion. PLoS Comput. Biol. *9*, e1003362.

Wang, Z., Liu, H., Gu, Y., and Chapman, E.R. (2011). Reconstituted synaptotagmin I mediates vesicle docking, priming, and fusion. J. Cell Biol. *195*, 1159–1170.

Wojcik, S.M., and Brose, N. (2007). Regulation of membrane fusion in synaptic excitation-secretion coupling: speed and accuracy matter. Neuron *55*, 11–24.

Xu, T., Rammner, B., Margittai, M., Artalejo, A.R., Neher, E., and Jahn, R. (1999). Inhibition of SNARE complex assembly differentially affects kinetic components of exocytosis. Cell *99*, 713–722.

Xu, J., Camacho, M., Xu, Y., Esser, V., Liu, X., Trimbuch, T., Pan, Y.Z., Ma, C., Tomchick, D.R., Rosenmund, C., and Rizo, J. (2017). Mechanistic insights into neurotransmitter release and presynaptic plasticity from the crystal structure of Munc13-1 C_1C_2BMUN. eLife *6*, e22567.

Xue, M., Ma, C., Craig, T.K., Rosenmund, C., and Rizo, J. (2008). The Janus-faced nature of the C(2)B domain is fundamental for synaptotagmin-1 function. Nat. Struct. Mol. Biol. *15*, 1160–1168.

Yavuz, H., Kattan, I., Hernandez, J.M., Hofnagel, O., Witkowska, A., Raunser, S., Walla, P.J., and Jahn, R. (2018). Arrest of *trans*-SNARE zippering uncovers loosely and tightly docked intermediates in membrane fusion. J. Biol. Chem. *293*, 8645–8655.

Zucker, R.S. (1989). Short-term synaptic plasticity. Annu. Rev. Neurosci. *12*, 13–31.